

**Reduction of
radiation biases by
downscaling
techniques**

S. Gimeno García et al.

This discussion paper is/has been under review for the journal Atmospheric Measurement Techniques (AMT). Please refer to the corresponding final paper in AMT if available.

Reduction of radiation biases by incorporating the missing cloud variability via downscaling techniques: a study using the 3-D MoCaRT model

S. Gimeno García^{1,2}, T. Trautmann¹, and V. Venema³

¹DLR – German Aerospace Center, Remote Sensing Technology Institute, Oberpfaffenhofen, 82234 Weßling, Germany

²TUM – Technical University of Munich, 80333 München, Germany

³University of Bonn, 53012 Bonn, Germany

Received: 2 January 2012 – Accepted: 30 January 2012 – Published: 14 February 2012

Correspondence to: S. Gimeno García (sebastian.gimenogarcia@dlr.de)

Published by Copernicus Publications on behalf of the European Geosciences Union.

Title Page

Abstract

Introduction

Conclusions

References

Tables

Figures

⏪

⏩

◀

▶

Back

Close

Full Screen / Esc

Printer-friendly Version

Interactive Discussion

Abstract

To handle complexity to the smallest detail in atmospheric radiative transfer models is in practice unfeasible. On the one hand, the properties of the interacting medium, i.e. the atmosphere and the surface, are only available at a limited spatial resolution.

5 On the other hand, the computational cost of accurate radiation models accounting for three-dimensional heterogeneous media are prohibitive for some applications, esp. for climate modeling and operational remote sensing algorithms. Hence, it is still common practice to use simplified models for atmospheric radiation applications.

10 Three-dimensional radiation models can deal with much more complexity than the one-dimensional ones providing a more accurate solution of the radiative transfer. In turn, one-dimensional models introduce biases to the radiation results.

15 With the help of stochastic models that consider the multi-fractal nature of clouds, it is possible to scale cloud properties given at a coarse spatial resolution down to a finer resolution. Performing the radiative transfer within the spatially fine-resolved cloud fields noticeably helps to improve the radiation results.

20 In the framework of this paper, we aim at characterizing cloud heterogeneity effects on radiances and broadband flux densities, namely: the errors due to unresolved variability (the so-called plane parallel homogeneous, PPH, bias) and the errors due to the neglect of transversal photon displacements (independent pixel approximation, IPA, bias). First, we study the effect of the missing cloud variability on reflectivities. We will show that the generation of subscale variability by means of stochastic methods greatly reduce or nearly eliminate the reflectivity biases. Secondly, three-dimensional broadband flux densities in the presence of realistic inhomogeneous cloud fields sampled at fine spatial resolutions are calculated and compared to their one-dimensional counterparts at coarser resolutions.

25

Reduction of radiation biases by downscaling techniques

S. Gimeno García et al.

Title Page

Abstract

Introduction

Conclusions

References

Tables

Figures



Back

Close

Full Screen / Esc

Printer-friendly Version

Interactive Discussion



1 Introduction

Clouds are the most complex objects of the Earth's atmosphere. However, their shape, extension and degree of inhomogeneity greatly depend on the cloud type. For instance, strongly convective clouds (e.g. cumulonimbus) are highly inhomogeneous, whereas boundary layer clouds (e.g. marine stratocumulus) appear to be nearly homogeneous. In broken cloudy skys, the radiation intensity is decreased by cloud blocking but also enhanced by reflection on cloud sides what leads to alternate shadowed and extra-illuminated regions on the surface.

Earth's average cloud cover fraction is approximately 62% (Rossow and Zhang, 1995), so a considerable part of the incoming and outgoing radiation is affected by clouds while traveling across the atmosphere. This fact lends clouds a distinguished place in Earth's radiation system: Clouds are recognized to be the main regulators of the radiation energy budget and, therefore, they are among the atmospheric constituents that affect most climate and weather. Moreover, clouds are a principal concern in remote sensing applications. Since the interaction of clouds with radiation is complex, observations contaminated with clouds are usually avoided when retrieving atmospheric molecular concentrations and surface properties. Further, even when clouds are the main goal of the observations, one-dimensional (1-D) approximate radiative transfer (RT) codes are used in the retrieval models.

To handle complexity to the smallest detail in RT models is in practice unfeasible. Two main reasons prevent from this: the optical properties of the Earth's atmosphere and surface are not available at an arbitrarily high resolution and time-consuming accurate models for solving the radiative transfer in three-dimensional resolved media are prohibitive for some applications, especially for climate modeling and operational remote sensing algorithms. Additionally, in some cases, the use of simplified models is justified because they deliver a exact solution and this has advantages in the inversion theory.

Reduction of radiation biases by downscaling techniques

S. Gimeno García et al.

Title Page

Abstract

Introduction

Conclusions

References

Tables

Figures



Back

Close

Full Screen / Esc

Printer-friendly Version

Interactive Discussion



Reduction of radiation biases by downscaling techniques

S. Gimeno García et al.

Title Page

Abstract

Introduction

Conclusions

References

Tables

Figures

⏪

⏩

◀

▶

Back

Close

Full Screen / Esc

Printer-friendly Version

Interactive Discussion



Three-dimensional (3-D) radiation models can account for much more complexity than one-dimensional (1-D) ones providing a more accurate solution of the radiative transfer at the cost of renouncing to the desirable exact mathematical solution and considerably increasing the calculation time.

Continuous technology progress has led to an increase of computing power, therefore more sophisticated models can be used, e.g. for radiative transfer computations (e.g. Evans, 1998; Barker et al., 2003; Buras and Mayer, 2011). Accordingly, many three-dimensional models have been developed to study cloud variability and its multi-fractal nature (e.g. Venema et al., 2006; Watson et al., 2009; Lovejoy et al., 2009; Bar-Or et al., 2011). Furthermore, quantity and quality of input data will be significantly improved with the launch of the Sentinel satellites in the framework of the European Global Monitoring for Environment and Security (GMES) program. So, the actual situation offers a perfect scenario to test the adequacy of the 1-D radiative transfer theory and opens the possibility to explore alternatives.

Stochastic models that combine cloud information at different spatial resolutions can be used to build a multi-scale view of clouds and express cloud properties at a large range of scales. Hence, the synergistic use of the cloud data at different spatial resolutions together with a stochastic cloud model would considerably improve the quality of the radiation fields.

In the framework of this paper, we aim at characterizing cloud heterogeneity effects on radiances, namely: The errors due to unresolved variability (the so-called plane parallel homogeneous, PPH, bias) and the errors due to the neglect of transversal photon displacements (independent pixel approximation, IPA, bias) (see e.g. Hinkelman et al., 2005). Firstly, 3-D radiative transfer simulations of nadir reflected radiances in the presence of realistic inhomogeneous cloud fields sampled at different spatial resolutions are going to be performed and compared. Secondly, the spectral flux densities integrated over the whole solar range will be computed for a diurnal cycle of an evolving cumulus at different resolutions and using different RT solvers. We will show that the fractally-consistent generation of subscale variability from the available cloud

properties at a coarse resolution by means of a stochastic cloud model (Venema et al., 2010) greatly reduces the biases in the radiative transfer.

In Sect. 2, we present the **Monte Carlo Radiative Transfer** (MoCaRT) model which was used to carry out all radiative transfer calculations throughout this paper. For the seek of validation, a comparison of MoCaRT with the I3RC-project “consensus” results is included in Sect. 2.1. The clouds fields used in this paper are presented in Sect. 3. In Sect. 4, we describe the methodology followed to study the effect of the missing variability on the radiative transfer. The results of the study are given in Sect. 5. In Sect. 6, we summarize the paper and draw some conclusions.

2 MoCaRT – Monte Carlo Radiative Transfer model

The Monte Carlo Radiative Transfer model (MoCaRT) is a flexible model designed to address different problems in atmospheric radiative transfer applications.

Its modular structure facilitates the software management and development, since the single parts of the code can be easily reused for new tasks. Further, the user interface is completely separated from the software, so that users do not have to know how the code is actually organized in order to carry out simulations.

MoCaRT has two main components implemented: the optical component and the radiation one. The optical block accounts for the calculation of optical properties from given atmospheric conditions of pressure, temperature, molecular abundances and/or cloud and aerosol microphysics. The surface albedo can be selected for different land compositions (Henderson-Sellers and Wilson, 1983). The solar irradiation can be calculated as the blackbody at Sun’s temperature or integrating solar measured or model spectra (Kurucz, 1995). The radiation block accounts for the radiative transfer through the optically active medium defined in the optical part.

MoCaRT offers the possibility of calculating the RT monochromatically, in narrow spectral intervals, or broadband. For monochromatic calculations, MoCaRT computes

Reduction of radiative biases by downscaling techniques

S. Gimeno García et al.

Title Page

Abstract

Introduction

Conclusions

References

Tables

Figures



Back

Close

Full Screen / Esc

Printer-friendly Version

Interactive Discussion



Reduction of radiation biases by downscaling techniques

S. Gimeno García et al.

Title Page

Abstract

Introduction

Conclusions

References

Tables

Figures

⏪

⏩

◀

▶

Back

Close

Full Screen / Esc

Printer-friendly Version

Interactive Discussion



the absorption coefficients via line-by-line from the HITRAN dataset, where line parameters for the main atmospheric coefficients are listed. In case of narrow intervals, effective absorption coefficients based on the mean interval transmittance are calculated. On request, a correlated k -distribution (CKD) approach for an arbitrary interval can be constructed. Broadband computations are performed via the CKD proposed by Fu and Liou (1992) adapted from SHDOM (Evans, 1998).

In order to calculate the optical properties of clouds and aerosols, the Mie theory can be applied. The Mie theory is a general description of the interaction of radiation with spherical particles. The wavelength of the incoming radiation and the particles size and composition (refractive index) are required to compute the scattering, absorption and extinction coefficient, as well as the scattering phase function. Bulk optical properties can be obtained by convolving the properties of individual particles with particle size distributions. Depending on the type of simulation that it is going to be carried out, the particle optical properties are spectrally averaged accordingly. Optionally, efficient parameterizations (but less accurate) can be used (Slingo, 1989; Stephens, 1994) in case of clouds, and (Shettle and Fenn, 1979; Hess et al., 1998) in case of aerosols.

MoCaRT can choose between several RT solvers depending on the radiation field of interest. From the point of view of how the variability is taken into account, four RT solvers are available. In the plane parallel homogeneous approximation (PPHA), all optical properties are averaged within vertical layers, whereas in the cloudy plane parallel homogeneous approximation (CPPHA), only cloudy optical properties are averaged within vertical layers and the radiation fields are computed combining the cloudy and the clear sky contributions using the cloud cover fraction (C_f) as the weight of the cloudy contribution and $(1 - C_f)$ as the weight of the clear sky one. The independent pixel/column approximation (IPA/ICA) (Cahalan et al., 1994) resolves the variability of the optical fields but the RT is calculated one-dimensionally in each atmospheric grid columns. A similar technique that considers independent columns along the solar illumination direction, the so-called tilted independent pixel approximation (TIPA) (Varnai and Davies, 1999) is also implemented. At last, the fully three-dimensional (3-D)

solution, where the optical properties are spatially resolved and the transversal photon transport is allowed, is also available.

In order to reach a fast and accurate convergence, several variance reduction and acceleration techniques have been implemented in MoCaRT. Here, we will describe briefly the diverse implemented techniques rather than go into details on the individual ones, since this would be the matter of a scientific paper by itself.

Usually, photon tracing, i.e. the randomly generation of photon trajectories, is the part of the code that consumes most of the computing time in Monte Carlo RT codes, and MoCaRT is not an exception. One-dimensional photon tracing algorithms are faster than their three-dimensional counterparts, since they do not have to account for photon horizontal location. Making use of this fact, it is possible to speed up the photon tracing process by considering a 3-D inhomogeneous atmosphere as if it would be one-dimensional. This goal is achieved by considering the maximum extinction coefficient values within vertical layers, $k_{\text{ext}}^{\text{max}}(z)$, and introducing a virtual interaction event that let photons unaltered. Assigning the probability weight of $k_{\text{ext}}(x, y, z)/k_{\text{ext}}^{\text{max}}(z)$ to the "maximum extinction" event and $(1 - k_{\text{ext}}(x, y, z)/k_{\text{ext}}^{\text{max}}(z))$ to the virtual scattering event, the photon tracing is unbiased. The method was described first by Marchuk et al. (1980). They considered the maximum values of the whole medium and called it maximum cross section method. Since we apply the method for a layered medium, it can be called the stratified maximum cross section method. This method works well when the maxima are not much larger than the extinction coefficients within layers. Special care has to be taken in case of different phase functions in the medium. We used this method for the flux density simulations presented in Sect. 4.2. In case of radiances, slower but more robust 3-D (or 2-D) tracing algorithms are used.

Several variance reduction methods are related to the manner that the photon-matter interactions are described in the model. The most intuitive method is to describe the history of single photons and their interaction with the medium as they behave in nature: they have constant energy, change direction after scattering events and disappear whenever an absorption event takes place. We refer to this method as "direct". Another

Reduction of radiation biases by downscaling techniques

S. Gimeno García et al.

Title Page

Abstract

Introduction

Conclusions

References

Tables

Figures

⏪

⏩

◀

▶

Back

Close

Full Screen / Esc

Printer-friendly Version

Interactive Discussion

In order to accelerate convergence, a method similar to Barker et al. (2003) is implemented.

2.1 Validation

In order to validate the MoCaRT model, in this section we present some comparison of radiative transfer simulations using MoCaRT and the consensus results of the Intercomparison of Three-Dimensional Radiation Codes (I3RC) project (Cahalan et al., 2005).

The I3RC project was conceived with the goal of comparing a wide variety of three-dimensional radiative transfer models applied to Earth's atmosphere. During the phase I of the project, several baselines for 3-D radiative transfer computations through inhomogeneous clouds were defined. These computations are based upon three cloud cases: a 1-D academic "step" cloud field, a 2-D field derived from radar and microwave observations of the *Atmospheric Radiation Measurement* (ARM) program, and a 3-D field derived from radiances measured by the Landsat 5 Thematic Mapper instrument. We performed the simulations suggested in phase I of I3RC and some selected results of flux densities and radiances are presented next.

Intercomparison of Three-dimensional Radiation Codes (I3RC)

The first case of the phase I of the I3RC project is a one-layer "step cloud" consisting of 32 pixels along the horizontal dimension. The first 16 pixels have an optical depth of 2 and the remaining ones of 18, resulting in a domain-average optical depth of 10. The horizontal extension of the cloud is of 0.5 km, whereas the vertical one is of 0.25 km everywhere, i.e. a flat cloud. This case allows for testing the model behaviour around a region with large optical depth gradient, i.e. the sharp transition from low to high cloud optical depth (see http://i3rc.gsfc.nasa.gov/input/step_cloud/index.html for detail).

The second case consists of a 2-D cloud field based on extinction retrievals from the combined measurements of the Millimeter Cloud Radar (MMCR) and the Microwave

Reduction of radiation biases by downscaling techniques

S. Gimeno García et al.

Title Page

Abstract

Introduction

Conclusions

References

Tables

Figures

⏪

⏩

◀

▶

Back

Close

Full Screen / Esc

Printer-friendly Version

Interactive Discussion



Radiometer (MWR) at the Atmospheric Radiation Measurement (ARM) CART site in Lamont, Oklahoma. The field consists of 640 columns along the horizontal axis. The horizontal width of the columns is of 50 m according to the measurement integration time (10 s) and the observed wind speed ($\sim 5 \text{ m s}^{-1}$). Vertically, the columns are resolved into 54 layers of 45 m thick each and extends from circa 0.6 km to 2.43 km above the Earth's surface (see http://i3rc.gsfc.nasa.gov/input/MMCR/high_res/020898/index.html for detail).

The third case is based on a two-dimensional (2-D) cloud field extracted from a Landsat-4 scene. The optical depth field consists of 128×128 vertically homogeneous horizontal columns. The column width is 30 m in both horizontal directions. In order to build up a three-dimensional (3-D) spatial cloud field, a constant cloud bottom at 0.2 km was considered and cloud top heights were determined from a separated field of geometrical thicknesses. The cloud fraction is 0.884 and the domain-average cloud optical depth (i.e. considering only the cloudy regions) is 11.4 (see <http://i3rc.gsfc.nasa.gov/input/Landsat/index.html> for detail).

Many institutions took part in the I3RC project contributing with different models. Combining the results of the best models, the so-called "consensus" results have been created and made available at the website of the I3RC project. We compare here the MoCaRT with the I3RC consensus results for the seek of validation.

Figure 1 shows a comparison of RT results for cases 1 and 2. Both clouds were considered to extend to infinity along the horizontal y-direction. No atmospheric effect was considered. The surface was black, i.e. the surface albedo was set to zero, except for the experiment 5 of case 2 (middle upper subplot) where it was set to 0.4. The Henyey-Greenstein scattering phase function with an asymmetry parameter of 0.85 was assumed throughout the cloud for all cases except for the experiment 7 of case 2 (right upper subplot), where the C1 scattering phase function (Deirmendjian, 1964) was used. The single scattering albedo, i.e. the ratio of the scattering to the extinction coefficient, was set to the unity (pure scattering) for all cases except for the experiment 4 of cases 1 and 2 (left and right lower subplots). The sun was overhead for both

Reduction of radiation biases by downscaling techniques

S. Gimeno García et al.

Title Page

Abstract

Introduction

Conclusions

References

Tables

Figures

⏪

⏩

◀

▶

Back

Close

Full Screen / Esc

Printer-friendly Version

Interactive Discussion



Reduction of radiation biases by downscaling techniques

S. Gimeno García et al.

Title Page

Abstract

Introduction

Conclusions

References

Tables

Figures

⏪

⏩

◀

▶

Back

Close

Full Screen / Esc

Printer-friendly Version

Interactive Discussion



cases of the central column and oblique with a solar zenith angle of 60° for the cases shown in the left and right columns. The upper row shows radiances and the lower row presents flux densities. The transmissivities and reflectivities were calculated for zenith and nadir view directions. The local discrepancies in reflectivities and transmissivities are few percent for all cases, except for the transmissivity of the experiment 7 of case 2, where the discrepancies exceed 5 % in some regions. In case 1, there are discrepancies in the transition regions from low to high optical depth and vice versa. The reason for these discrepancies is because we calculated the radiances at the centre of the pixels and not averaged over the whole pixel. The relative differences in case of reflectances and transmittances are lower than 1 %. All cases are well within the error bars as illustrated in the upper panels. The domain averaged quantities agree better than 1 ‰.

Figure 2 shows the comparison results relative to case 3. Since in this case the extinction field is three-dimensional, it is necessary to compare the two-dimensional radiative quantities in separate graphs. The upper subplots present reflectivity results and the lower ones absorptance. The surface albedo was set to zero and the Henyey-Greenstein scattering phase function with an asymmetry parameter of 0.85 was assumed throughout the cloud for both experiments, 1 and 4. The single scattering albedo was 1 and 0.99, respectively. The solar zenith angle was set to 0° (upper row) and 60° (lower row). Although the extinction field is highly variable and the solar illumination is not perpendicular, the figures provided by both methods seem to be twins. The mean, maximal and minimal values agree better than 0.1 %, which is clearly better than the required accuracy in the I3RC project.

3 Cloud fields

In this section, we present the three-dimensional inhomogeneous cloud fields that have been used in this paper as a framework for the study of the cloud variability effect on the radiative transfer.

Reduction of radiation biases by downscaling techniques

S. Gimeno García et al.

[Title Page](#)[Abstract](#)[Introduction](#)[Conclusions](#)[References](#)[Tables](#)[Figures](#)[Back](#)[Close](#)[Full Screen / Esc](#)[Printer-friendly Version](#)[Interactive Discussion](#)

Venema et al. (2010) developed a downscaling algorithm for cloud fields, that generates high-resolution 3-dimensional cloud fields based on coarse resolution cloud water and cloud cover fields. This algorithm generates clouds with realistic subscale variability that complements the resolved cloud field and makes radiative transfer computations more accurate. This statement can be tested, if we take the coarse-resolved (400 × 400 m) cloud set as the starting point, generate cloud variability down to a resolution of 40 × 40 m, and compare the results with the original cloud set, also of 40 × 40 m horizontal resolution, from which the coarse-resolved cloud set was calculated.

In the next subsections, we describe in detail the two studies for investigating the effects of the missing variability on radiances and flux densities.

4.1 Effect of missing variability on radiances

Radiance observations by sensors on-board of spacecraft and aircraft platforms or on ground-based stations can be used to obtain information about the thermodynamic state of the atmosphere, including the content of the main atmospheric molecules, cloud condensates and aerosols. In general, the signal measured by atmospheric sensors have contributions from a large portion of the atmosphere, where the probability of containing cloud condensates is high. It is common practice in atmospheric composition remote sensing to filter out the cloudy scenes or to neglect cloudiness below a certain threshold (e.g. for cloud cover fractions below 5 %). Other algorithms consider the clouds as homogeneous blocks that cover a fraction of the observed scene and the rest of the scene as clear sky. In these cases, cloud variability is suppressed within the cloud fields and the photon transport from the cloudy to the clear sky region is not allowed.

For surface remote sensing applications, sensors are provided with a much higher spatial resolution than their atmospheric counterparts. Cloud masking algorithms are used to filter out cloudy pixels, but in case of thin clouds (e.g. cirrus) or clouds over bright surfaces (e.g. ice or desert areas), these algorithms may fail. In order to retrieve

surface properties, atmospheric effects have to be corrected. Surface retrieval algorithms work at high spatial resolution but the transversal photon transport is not allowed.

These limitations imposed to the radiative transfer solvers introduce biases to the radiation solutions, and consequently, also biases to the retrieval results.

Here, we present a study on the effect of the spatial resolution on measured reflectivities and propose a method for improving the results. Let us assume that we have defined the cloud properties at a horizontal resolution of 400×400 m. We will refer to this clouds as “coarse” fields. Additionally, by means of the downscaling method presented in Venema et al. (2010), we produced a new cloud set with horizontal variability down to 40×40 m. The downscaling method accepts measured in addition to academic power spectra of cloud properties, allowing to descend to a smaller spatial scale in a realistic manner. In most of the cases, we do not have the possibility to check if the generated variability is correct, unless we observe the same cloudy scene with sensors of different resolution or we model the same scene at different resolutions. However, in our case study, we use the cumulus clouds of Sect. 3 as reference and the radiation results can be directly compared to them. Hence, deviation of the reflectivities from the original cloud set will be interpreted as biases and, accordingly, we can test the impact of the spatial resolution as well as the proposed improvement method by generating the missing variability. For a detailed explanation of the downscaling method we refer to Venema et al. (2010).

Since this study is focused on the cloud spatial variability, we did not considered any atmospheric effect, i.e. the cloud fields were embedded in vacuum, neither molecular absorption or scattering was considered, nor aerosol extinction. Lambertian reflection at the flat surface with an albedo of 0.1 was considered. The cloud scattering properties were calculated by means of the parameterization proposed by Slingo (1989). The phase function was approximated by the Henyey-Greenstein phase function with the asymmetry parameter calculated from the aforementioned parameterization. Two solar zenith angles were considered, 0° and 60° . The reflectivities were calculated for a nadir

Reduction of radiation biases by downscaling techniques

S. Gimeno García et al.

Title Page

Abstract

Introduction

Conclusions

References

Tables

Figures



Back

Close

Full Screen / Esc

Printer-friendly Version

Interactive Discussion



viewing instrument. The same simulations were repeated for all 49 cloudy scenes of all three cloud sets: the coarse, the downscaled and the reference one.

Figures 4 and 5 illustrate scene reflectivities randomly selected from all cloud cases for solar zenith angles of 0° and 60° , respectively. The upper row presents the reflectivities computed in the original cloud set which will be considered here as the real cloudy conditions. The reflectivities computed in the coarsened cloud fields are presented in the central row, where the lack of small detail is manifest. The lower row presents the reflectivities in the cloud fields with generated variability. One can see that the reflectivities resemble the ones of the original fields, indicating the convenience of calculating the radiative transfer at spatially fine-resolved cloud fields. Notice the realistic shadows of the cloud fields on the ground in Fig. 5. In this illustration, the oblique sun is illuminating from the South.

In Sect. 5.1 domain averaged reflectivities are analyzed.

4.2 Effect of missing variability on flux densities: a diurnal cycle

Together with the impact of cloud variability on radiances, we also investigate the effect on flux densities. In particular, we have studied the impact on flux densities integrated over the whole solar region of the spectrum. Thermal radiation was not considered. The designed scenario for this study is presented next.

The diurnal cycle of the convective cumulus presented in Sect. 3 (see Fig. 3) was embedded into a model atmosphere over land. Only the troposphere and the lower stratosphere (top of the atmosphere was set at 30 km) were considered. The cloud optical properties were calculated from the microphysical properties by means of the parameterization proposed by Slingo (1989). The angular distribution of cloud scattering events was described by the Henyey-Greenstein phase function with the asymmetry parameter obtained previously from the mentioned parameterization. The solar position (zenith and azimuth) was exactly calculated as a function of time and geolocation (see details in Sect. 3). The broadband molecular absorption was taken into account by means of the correlated k -distribution (CKD) given by Fu and Liou (1992).

Reduction of radiation biases by downscaling techniques

S. Gimeno García et al.

Title Page

Abstract

Introduction

Conclusions

References

Tables

Figures



Back

Close

Full Screen / Esc

Printer-friendly Version

Interactive Discussion



**Reduction of
radiation biases by
downscaling
techniques**

S. Gimeno García et al.

[Title Page](#)[Abstract](#)[Introduction](#)[Conclusions](#)[References](#)[Tables](#)[Figures](#)[⏪](#)[⏩](#)[◀](#)[▶](#)[Back](#)[Close](#)[Full Screen / Esc](#)[Printer-friendly Version](#)[Interactive Discussion](#)

Molecular (Rayleigh) scattering coefficients were calculated by the formula given by Nicolet (1984) and averaged over the broadband intervals of the k -distribution. The effect of aerosols was neglected. Lambertian reflection at the surface was considered with a broadband surface albedo corresponding to an agricultural region (Henderson-Sellers and Wilson, 1983).

The RT simulations were performed using the Monte Carlo Radiative Transfer model (MoCaRT), which can provide both, the 3-D exact solution of the RT or an approximate one by employing a variety of 1-D methods. The radiation simulations comprised the whole solar range.

On the one hand, we carried out fully 3-D calculations over the whole day using the fine resolved cumuli ($100\text{ m} \times 100\text{ m} \times 40\text{ m}$) and considered the results of these simulations as reference (“the truth”). On the other hand, we calculated the RT by means of the independent column approximation (ICA) using coarser clouds, representing the RT scheme in a cloud resolving model with coarser spatial resolution. In this case, the cumulus clouds were horizontally coarsened to 16 by 16 pixels (i.e. the resolution was decreased four-fold down to $400\text{ m} \times 400\text{ m} \times 40\text{ m}$).

5 Results

Domain-averaged results of the studies presented in Sect. 4 are shown here. The results are presented separately: first, we compare the reflectivities of the coarse and the downscaled clouds with the reference ones; secondly, we compare the flux densities of the coarse cumulus clouds with the reference ones during the diurnal cycle.

5.1 Reflectivity: difference plots

Figure 6 shows difference plots of domain-averaged reflectivities between the coarse and the reference clouds (left panel) and the downscaled and the reference clouds (right panel) for a solar zenith angle of 0° . The abscissas axis indicates the mean

reflectivity of the reference clouds and the ordinates axis indicates the relative differences. The blue dots represent the differences within a single cloudy scene and the error bars the corresponding standard deviations. The solid red line represents the mean bias of all cloud fields and the dashed red lines, the mean plus and minus the standard deviation, respectively. Fully 3-D RT calculations were performed in all cases, so the reflectivities differences cannot be attributed to restrictions in the radiative transfer, but entirely to the resolution at which the optical properties are defined. The loss of variability leads to an overestimation of the reflected flux density in case of the coarse-resolved clouds due to Jensen's inequality (see left panel). The higher the reflectivities (i.e. higher optical depths), the higher the differences between the coarse clouds and the reference ones. The mean bias introduced only by defining the cloud fields at a coarser resolution is about 40 %. If cloud variability is generated by means of stochastic methods and added to the coarse clouds, this bias is eliminated (see right panel).

Figure 7 is equivalent to Fig. 6 except that in this case the solar zenith angle was set to 60°. The same conclusions found in Fig. 6 hold for oblique illumination. The mean bias due to the lack of variability is of about 35 %. Again, the fractal generation of cloud subscale variability helps to eliminate the mean bias. In this case, the downscaled mean bias is about 1 %.

5.2 Flux densities: a diurnal cycle

We will study the errors made when calculating one-dimensionally the solar radiation flux densities within coarse-resolved cloudy atmospheres instead of resolving cloud horizontal variability and accounting for the photon horizontal transport.

Figure 8 shows the results of the study. The left panel shows the reflected flux densities at the top of the atmosphere (TOA), the right top panel shows the transmitted flux densities at Earth's surface and the right bottom panel shows the absorbed power through the whole atmosphere. Note that the absolute values of the flux densities depend on the incoming solar radiation which is a function of the cosine of the solar zenith angle (SZA), what is clearly seen in all three plots.

Reduction of radiation biases by downscaling techniques

S. Gimeno García et al.

Title Page

Abstract

Introduction

Conclusions

References

Tables

Figures

⏪

⏩

◀

▶

Back

Close

Full Screen / Esc

Printer-friendly Version

Interactive Discussion



Reduction of radiation biases by downscaling techniques

S. Gimeno García et al.

[Title Page](#)[Abstract](#)[Introduction](#)[Conclusions](#)[References](#)[Tables](#)[Figures](#)[⏪](#)[⏩](#)[◀](#)[▶](#)[Back](#)[Close](#)[Full Screen / Esc](#)[Printer-friendly Version](#)[Interactive Discussion](#)

Two effects mainly contribute to the differences in the flux densities. First, cloud variability is described at different resolutions, and second, horizontal photon transport is allowed in one case and forbidden in the other. The loss of variability leads to an overestimation of the reflected flux densities in case of the coarse resolved clouds due to Jensen's inequality (ICA-PPA bias). ICA simulations neglect the radiative communication between atmospheric columns (3-D-ICA bias). This bias depends on the spatial distribution of cloud properties as well as on the illumination geometry.

In our study, the ICA-coarse (green spots) reflected flux densities are larger than their 3-D-fine counterparts (blue spots) over the whole day with maxima as large as 30 W m^{-2} . The standard deviation of the mean is shown as error bars: the larger the error bars, the higher the dispersion of the values. As a consequence of horizontal transport, 3-D-fine reflected flux densities at TOA are smoother than the ICA-coarse ones. In case of transmitted flux densities at the ground, 3-D-fine fields still show large variability, since the cloud layers are close to the surface.

6 Conclusions and outlook

In highly inhomogeneous cloudy atmospheres, the radiative transfer strongly depends on the horizontal scale at which the microphysical properties of the cloud fields are defined. The neglect of cloud variability introduces biases while simulating the radiation transfer. These biases affect the accuracy of remote sensing applications and climate and weather prediction models.

Reflectivities are important radiation quantities for remote sensing. We studied the effect that cloud resolution has on reflectivities. We showed that considering the cloud properties at a horizontal resolution of 400 m by 400 m introduces a bias of about 40 % for overhead sun and 35 % for a solar zenith angle of 60° when averaging over 49 cumulus scenes of different cloudiness in comparison to a resolution of 40 m by 40 m. Additionally, we showed that generating subscale variability by means of stochastic

methods and adding this variability to the coarse fields greatly improves the reflectivity result eliminating the biases.

The neglect of the subscale variability introduces large biases in the radiation fields. For radiation flux densities integrated over the whole solar range, these biases can reach the magnitude of tens of W m^{-2} for reflection (albedo) and transmission, and few W m^{-2} for absorption. The magnitude of the biases compete with the other main sources of uncertainties in climate and weather prediction model.

Understanding the multi-scale interaction of radiation with heterogeneous cloud fields will help to improve the retrieval of atmospheric constituents. The GMES (Global Monitoring for Environment and Security) satellites will supply upgraded data of the Earth's surface and atmosphere. The quality and quantity of the GMES data will provide a deeper insight of the atmosphere but will also pose some challenges to the processing of the data. In addition to the cloud properties retrieval, which will directly profit from a better description of cloud-radiation interaction, other atmospheric retrievals will also benefit. In particular, the quality of atmospheric gas retrievals greatly depends on the treatment of cloud information, either directly (e.g. cloud cover and cloud top height) or indirectly (e.g. cloud masking). Hence, a realistic description of clouds will particularly be useful for gas retrievals.

Currently, there are several sensor constellations mounted on the same spacecraft platform that provide cloud information at different resolutions. Three of such constellations are MERIS and SCIAMACHY on Envisat; AVHRR, GOME2 and IASI on MetOp; and CAI and TANSO on GOSAT. By means of stochastic methods, cloud information at different resolutions can be optimally combined to create a multi-scale view of the clouds. A better understanding of cloud structure on wide-footprint scenes, will not only imply an enhancement of the quality but also of the quantity of the data. For instance, in the methane and carbon dioxide retrievals with GOSAT only cloud-free observations are used. This reduces the useful data for climate-relevant gases retrieval to ca. 2%–5% of the total. Additionally, three-dimensional radiative transfer models can supply valuable information. On the one hand, 3-D-RT models can be used to estimate

Reduction of radiation biases by downscaling techniques

S. Gimeno García et al.

Title Page

Abstract

Introduction

Conclusions

References

Tables

Figures



Back

Close

Full Screen / Esc

Printer-friendly Version

Interactive Discussion



the limitations of the one-dimensional theory implemented in the retrieval algorithms. On the other hand, they describe the cloud-radiation interaction more precisely and can provide add-on products (i.e. photon path length statistics) that will improve the retrievals.

- 5 *Acknowledgements.* We would like to thank the Intercomparison of Three-dimensional Radiation Codes (I3RC) project for making available their results which we used for the validation of our radiative transfer model MoCaRT. We are specially thankful to Tamás Várnai for his assistance during the results interpretation.

References

- 10 Bar-Or, R. Z., Altaratz, O., and Koren, I.: Global analysis of cloud field coverage and radiative properties, using morphological methods and MODIS observations, *Atmos. Chem. Phys.*, 11, 191–200, doi:10.5194/acp-11-191-2011, 2011. 1546
- Barker, H., Goldstein, R., and Stevens, D.: Monte carlo simulation of solar reflectances for cloudy atmospheres, *J. Atmos. Sci.*, 60, 1881–1894, 2003. 1546, 1551
- 15 Brown, A. R., Cederwall, R. T., Chlond, A., Duynkerke, P. G., Golaz, J. C., Khairoutdinov, M., Lewellen, D. C., Lock, A. P., MacVean, M. K., Moeng, C. H., Neggers, R. A. J., Siebesma, A. P., and Stevens, B.: Large-eddy simulation of the diurnal cycle of shallow cumulus convection over land, *Q. J. Roy. Meteorol. Soc.*, 128, 1075–1093, 2002. 1554, 1568
- Buras, R. and Mayer, B.: Efficient unbiased variance reduction techniques for monte carlo simulations of radiative transfer in cloudy atmospheres: The solution, *J. Quant. Spectrosc. Ra.*, 112, 434–447, 2011 1546
- 20 Cahalan, R., Ridgway, W., Wiscombe, W., and Gollmer, S.: Independent Pixel and Monte Carlo Estimates of Stratocumulus Albedo, *J. Atmos. Sci.*, 51, 3776–3790, 1994. 1548
- Cahalan, R. F., Oreopoulos, B., Davies, R., Ackerman, T. P., Barker, H. W., Clothiaux, E. E., Ellingson, R. G., Garay, M. J., Kassianov, E., Kinne, S., Macke, A., O’Hirok, W., Partain, P. T., Prigarin, S. M., Rublev, A. N., Stephens, G. L., Szczap, F., Takara, E. E., Vanai, T., Wen, G., and Zhuravleva, T. B.: The i3rc - bringing together the most advanced radiative transfer tools for cloudy atmospheres, *B. Am. Meteorol. Soc.*, 86, 1275–1293, doi:10.1175/BAMS-86-9-1275, 2005. 1551
- 25

Reduction of radiation biases by downscaling techniques

S. Gimeno García et al.

Title Page

Abstract

Introduction

Conclusions

References

Tables

Figures



Back

Close

Full Screen / Esc

Printer-friendly Version

Interactive Discussion



Reduction of radiation biases by downscaling techniques

S. Gimeno García et al.

Title Page

Abstract

Introduction

Conclusions

References

Tables

Figures

⏪

⏩

◀

▶

Back

Close

Full Screen / Esc

Printer-friendly Version

Interactive Discussion



- Deirmendjian, D.: Scattering and polarization properties of water clouds and hazes in the visible and infrared, *Appl. Optics*, 3, 187–196, 1964. 1552
- Evans, K. F.: The spherical harmonics discrete ordinate method for three-dimensional atmospheric radiative transfer, *J. Atmos. Sci.*, 55, 429–446, 1998. 1546, 1548
- 5 Fu, Q. and Liou, K. N.: On the correlated k-distribution method for radiative transfer in nonhomogeneous atmospheres, *J. Atmos. Sci.*, 49, 2139–2156, 1992. 1548, 1558
- Henderson-Sellers, A. and Wilson, M.: Surface albedo data for climatic modeling, *Rev. Geophys.*, 21, 1743–1778, 1983. 1547, 1559
- Hess, M., Koepke, P., and Schult, I.: Optical properties of aerosols and clouds: The software package opac, *B. Am. Meteorol. Soc.*, 79, 831–844, 1998. 1548
- 10 Hinkelman, L., Stevens, B., and Evans, K.: A large-eddy simulation study of anisotropy in fair-weather cumulus cloud fields, *J. Atmos. Sci.*, 62, 2155–2171, 2005. 1546
- Kurucz, R.: The solar spectrum: atlases and line identifications, in *Workshop on Laboratory and Astronomical High resolution Spectra*, *Astron. Soc. of the Pac. Conf. Ser.*, vol. 81, 17–31, 1995. 1547
- 15 Lovejoy, S., Watson, B., Grosdidier, Y., and Schertzer, D.: Scattering in thick multifractal clouds, part ii: Multiple scattering, *Physica A*, 388, 3711–3727, 2009. 1546
- Marchuk, G., Mikhailov, G., and Nazarialiev, M.: *The Monte Carlo methods in atmospheric optics*, Springer Series in Optical Sciences, 1980. 1549, 1550
- 20 Nicolet, M.: On the molecular scattering in the terrestrial atmosphere: An empirical formula for its calculation in the homosphere, *Planet. Space Sci.*, 32, 1467–1468, 1984. 1559
- Rossow, W. and Zhang, Y.-C.: Calculation of surface and top of the atmosphere radiative fluxes from physical quantities based on ISCCP data sets 2. Validation and first results, *J. Geophys. Res.*, 100, 1167–1197, 1995. 1545
- 25 Shettle, E. P. and Fenn, R. W.: *Models for the aerosols of the lower atmosphere and the effects of humidity variations on their optical properties*, Tech. rep., Air Force Geophysics Lab. Hanscom AFB, MA, Optical Physics Div., 1979. 1548
- Slingo, A.: A GCM parameterization for the shortwave radiative properties of water clouds, *J. Atmos. Sci.*, 46, 1419–1427, 1989. 1548, 1557, 1558
- 30 Stephens, G.: *Remote sensing of the lower atmosphere*, Oxford University Press, New York, NY, USA, 1994. 1548
- Varnai, T. and Davies, R.: Effects of cloud heterogeneities on shortwave radiation: Comparison of cloud-top variability and internal heterogeneity, *J. Atmos. Sci.*, 56, 4206–4224, 1999. 1548

**Reduction of
radiation biases by
downscaling
techniques**

S. Gimeno García et al.

Title Page

Abstract

Introduction

Conclusions

References

Tables

Figures

I◀

▶I

◀

▶

Back

Close

Full Screen / Esc

Printer-friendly Version

Interactive Discussion



- Venema, V., Meyer, S., García, S., Kniffka, A., Simmer, C., Crewell, S., Löhnert, U., Trautmann, T., and Macke, A.: Surrogate cloud fields generated with the iterative amplitude adapted fourier transform algorithm, *Tellus A*, 58, 104–120, 2006. 1546
- 5 Venema, V., Gimeno Garcia, S., and Simmer, C.: A new algorithm for the downscaling of cloud fields, *Q. J. Roy. Meteorol. Soc.*, 136, 91–106, 2010. 1547, 1556, 1557
- Watson, B., Lovejoy, S., Grosdidier, Y., and Schertzer, D.: Scattering in thick multifractal clouds, part i: Overview and single scattering, *Physica A*, 388, 3695–3710, 2009. 1546

Reduction of radiation biases by downscaling techniques

S. Gimeno García et al.

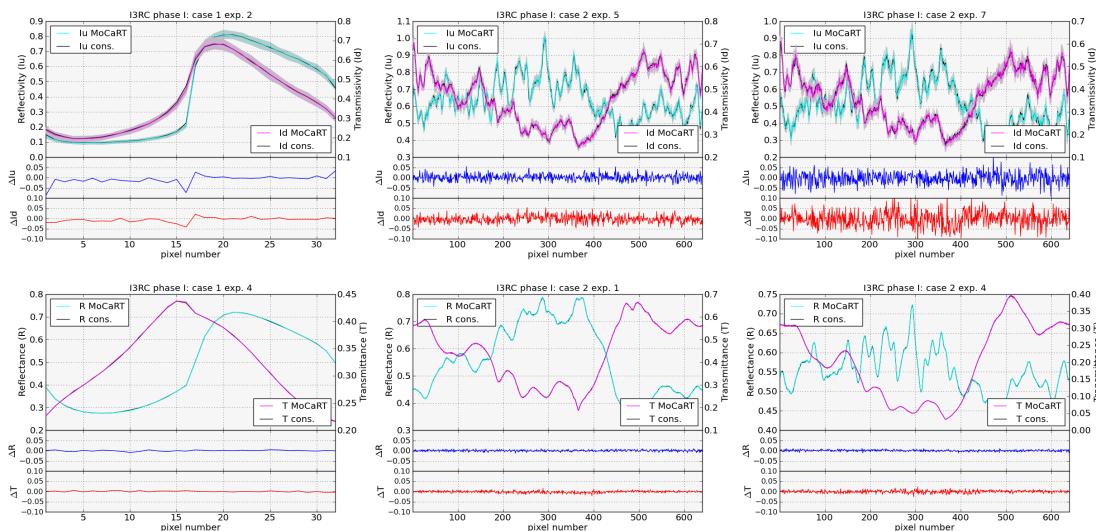


Fig. 1. I3RC project phase I. Case 1 represents a step cloud of mean optical thickness of 10. Case 2 represents a measured 2-D cloud field. MoCaRT results are compared to the consensus results of the participants in the I3RC project. The upper row presents radiance results (reflectivities and transmissivities), whereas the lower row presents flux densities (reflectances and transmittances). The left column illustrates results of the case 1 and the central and right column of case 2. The central (lower) panel of all subplots illustrates the reflectivity/reflectance (transmissivity/transmittance) relative difference. The local discrepancies are few percent for all cases, except for the transmissivity of experiment 7 of case 2, where the discrepancies exceed 5% in some regions. All cases are well within the error bars as illustrated in upper panels.

[Title Page](#)
[Abstract](#)
[Introduction](#)
[Conclusions](#)
[References](#)
[Tables](#)
[Figures](#)
[Back](#)
[Close](#)
[Full Screen / Esc](#)
[Printer-friendly Version](#)
[Interactive Discussion](#)

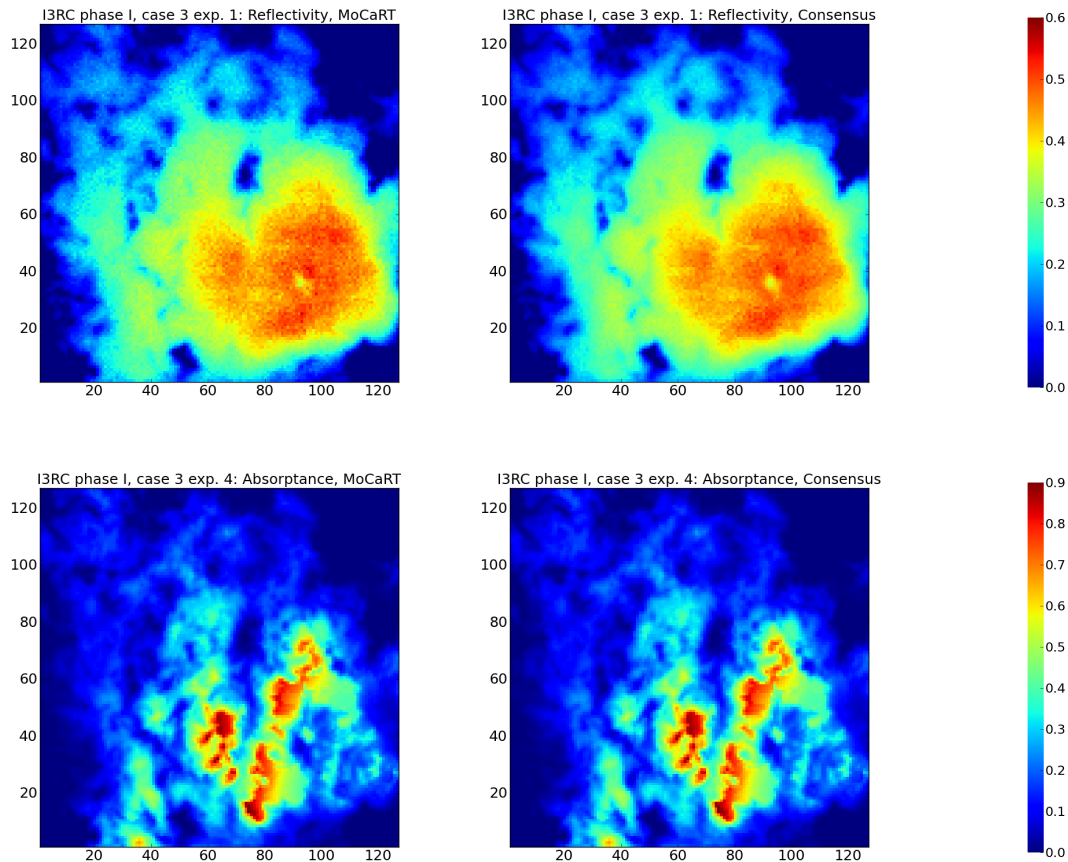


Fig. 2. I3RC project phase I. Case 3 represents a Landsat cloud. MoCaRT results are compared to the consensus results of the participants in I3RC project. The left column shows the MoCaRT and the right column, the consensus results. The top row illustrates reflectivity fields and the bottom one absorptance. Differences are well within the Monte Carlo noise.

Reduction of radiation biases by downscaling techniques

S. Gimeno García et al.

Title Page

Abstract Introduction

Conclusions References

Tables Figures

⏪ ⏩

◀ ▶

Back Close

Full Screen / Esc

Printer-friendly Version

Interactive Discussion

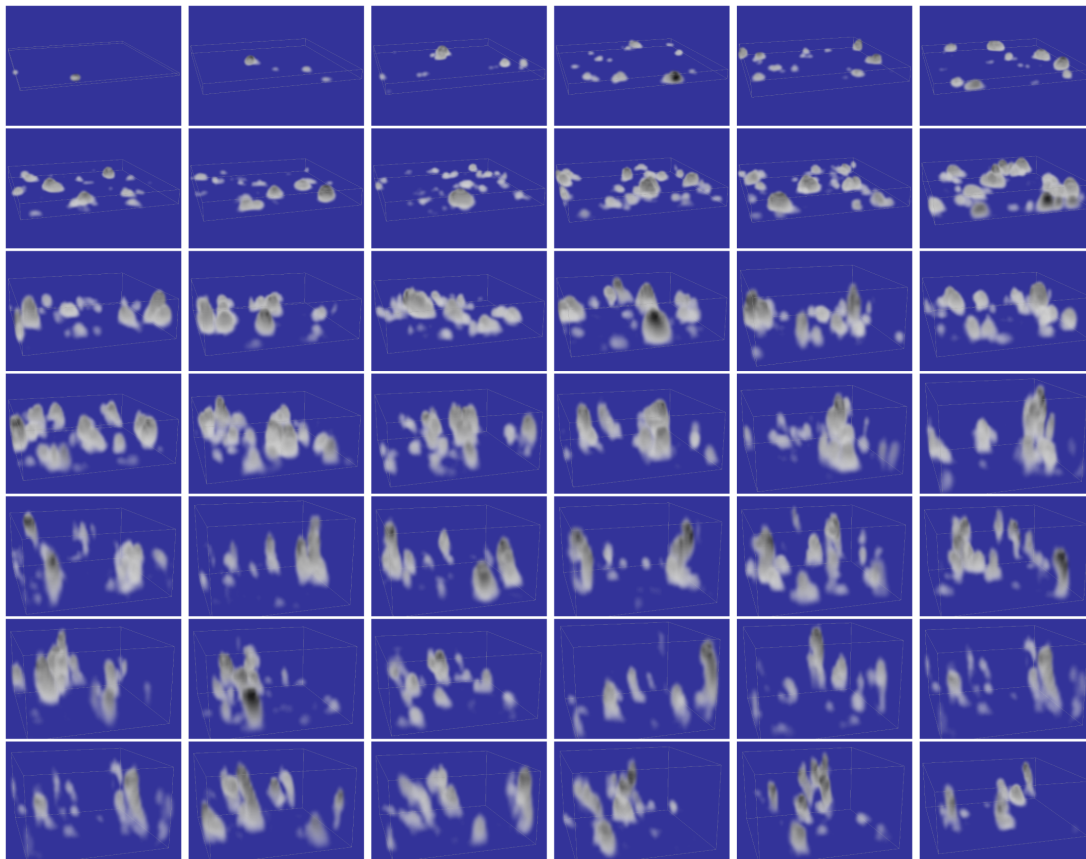


Fig. 3. Large eddy simulation of the diurnal cycle of shallow cumulus convection over SGP site of the ARM program (Brown et al., 2002). The snapshots represent the liquid water content fields (light/dark grey for low/high LWC) sampled each 20 min from 08:40 UTC until 22:20 UTC.

Reduction of radiation biases by downscaling techniques

S. Gimeno García et al.

Title Page

Abstract Introduction

Conclusions References

Tables Figures

◀ ▶

◀ ▶

Back Close

Full Screen / Esc

Printer-friendly Version

Interactive Discussion

Reduction of radiation biases by downscaling techniques

S. Gimeno García et al.

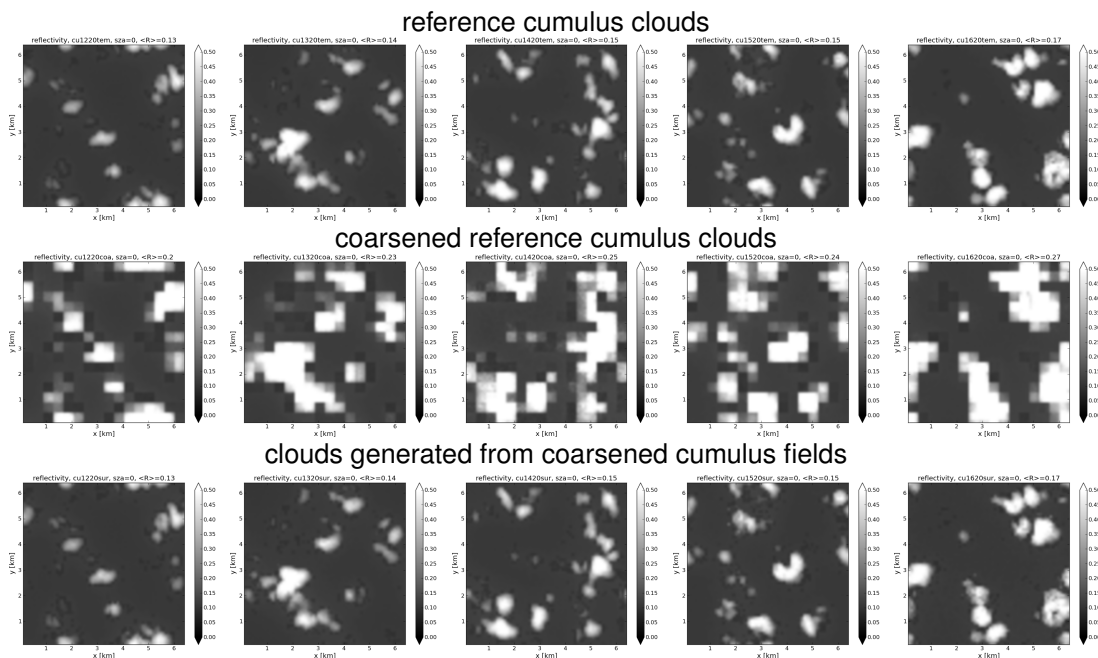


Fig. 4. Reflectivity fields of some selected scenes of the cumulus diurnal cycle presented in Sect. 3. The sun is overhead ($\text{SZA} = 0^\circ$) and the observer looks exactly in the nadir direction. The top row corresponds to the LES clouds considered here as the reference (see Fig. 3). The middle row represents the coarsened cloud reflectivities. The bottom row illustrates the reflectivities calculated at clouds generated from the coarsened ones by adding the missing sub-scale variability. Notice the similarity of the top and bottom row fields indicating the good job done by the downscaling model.

Title Page

Abstract

Introduction

Conclusions

References

Tables

Figures

⏪

⏩

◀

▶

Back

Close

Full Screen / Esc

Printer-friendly Version

Interactive Discussion

Reduction of radiation biases by downscaling techniques

S. Gimeno García et al.

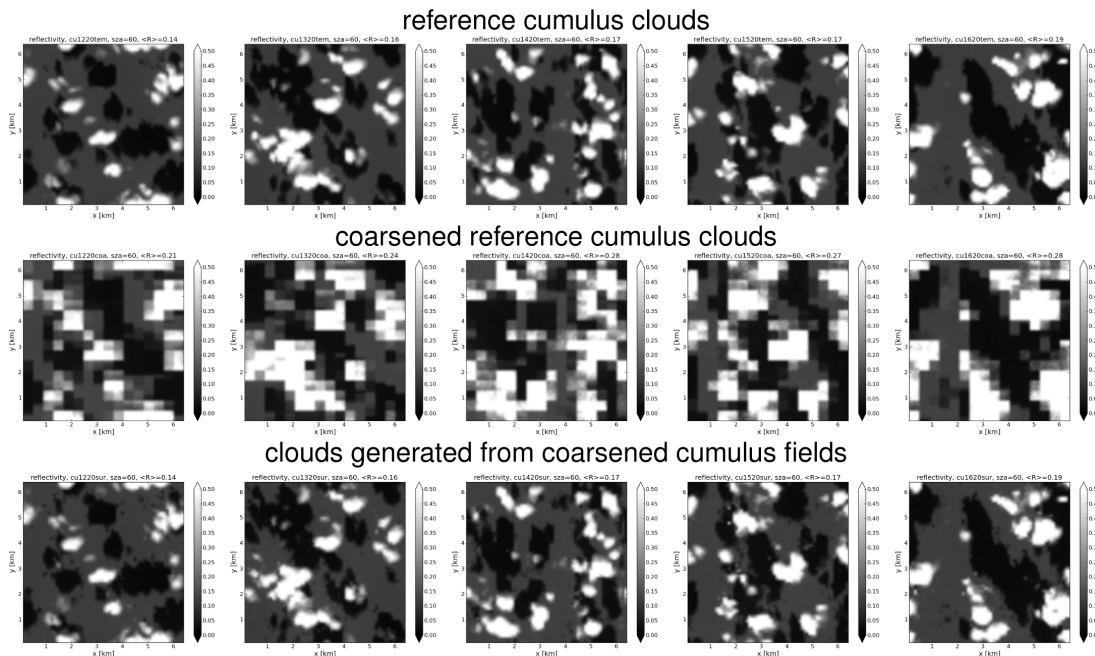


Fig. 5. Reflectivity fields of some selected scenes of the cumulus diurnal cycle presented in Sect. 3. The sun illuminates the scenes from the south at a zenith angle of 60° . The observer looks exactly in the nadir direction. The top row corresponds to the LES clouds considered here as the reference (see Fig. 3). The middle row represents the coarsened cloud reflectivities. The bottom row illustrates the reflectivities calculated at clouds generated from the coarsened ones by adding the missing sub-scale variability. Notice the similarity of the top and bottom row fields indicating the convenience of calculating the radiative transfer at spatially fine-resolved cloud fields.

[Title Page](#)
[Abstract](#)
[Introduction](#)
[Conclusions](#)
[References](#)
[Tables](#)
[Figures](#)
[◀](#)
[▶](#)
[◀](#)
[▶](#)
[Back](#)
[Close](#)
[Full Screen / Esc](#)
[Printer-friendly Version](#)
[Interactive Discussion](#)

Reduction of radiation biases by downscaling techniques

S. Gimeno García et al.

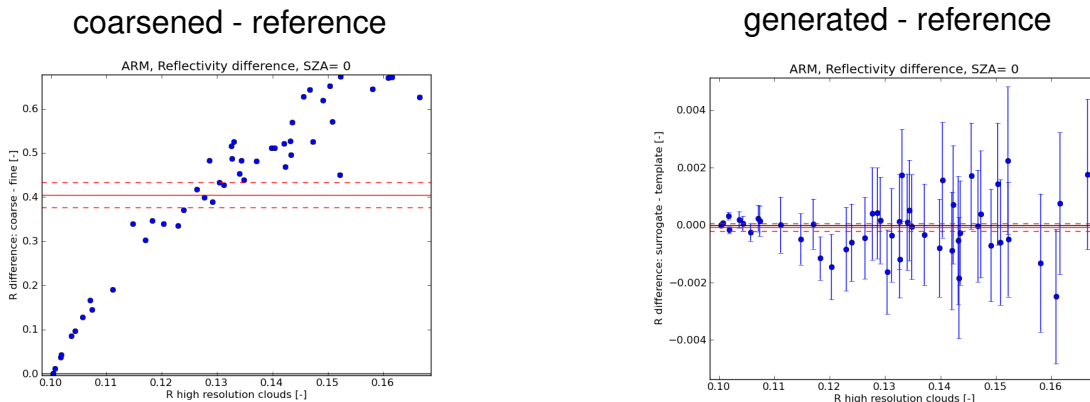


Fig. 6. Differences in domain-averaged reflectivity. The solar zenith angle was set to 0° . The abscissas axis indicates the mean reflectivity of the reference clouds and the ordinates axis indicates the relative differences. The blue dots represent the differences within a single cloudy scene and the error bars the corresponding standard deviations. The solid red line represents the mean bias of all cloud fields and the dashed red lines, the mean plus and minus the standard deviation, respectively.

[Title Page](#)
[Abstract](#)
[Introduction](#)
[Conclusions](#)
[References](#)
[Tables](#)
[Figures](#)
[⏪](#)
[⏩](#)
[◀](#)
[▶](#)
[Back](#)
[Close](#)
[Full Screen / Esc](#)
[Printer-friendly Version](#)
[Interactive Discussion](#)

Reduction of radiation biases by downscaling techniques

S. Gimeno García et al.

Title Page

Abstract

Introduction

Conclusions

References

Tables

Figures

⏪

⏩

◀

▶

Back

Close

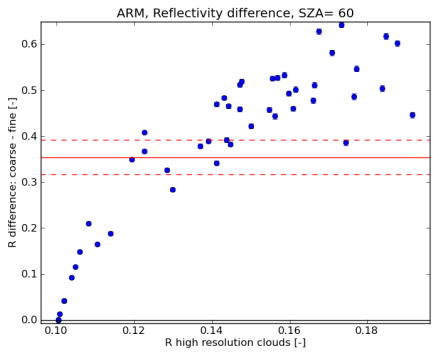
Full Screen / Esc

Printer-friendly Version

Interactive Discussion



coarsened - reference



generated - reference

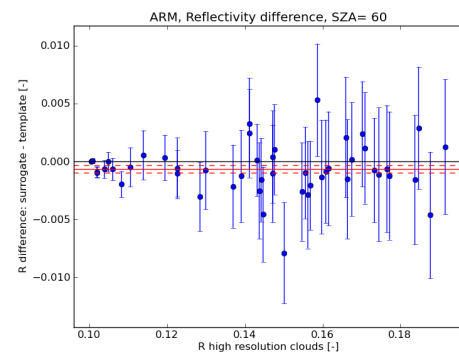


Fig. 7. Same as Fig. 6 but for a solar zenith angle of 60°.

Reduction of radiation biases by downscaling techniques

S. Gimeno García et al.

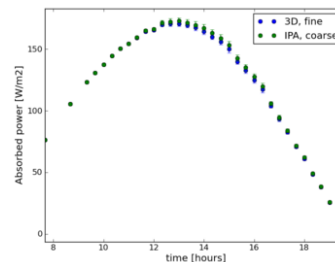
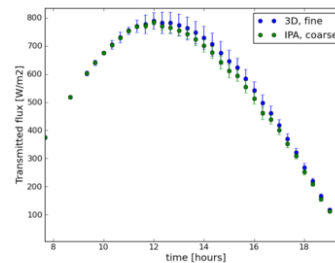
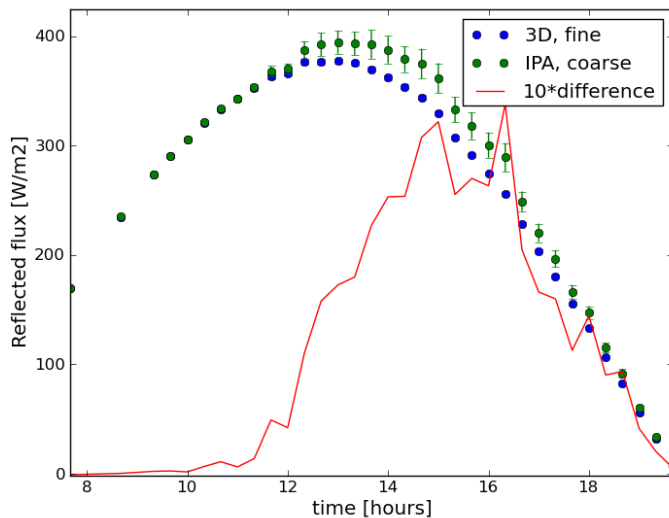


Fig. 8. Radiation fields in a diurnal cycle of shallow cumulus clouds developing over land (see Fig. 3). The left panel shows the reflected flux density at the top of the atmosphere, the right top panel, the transmitted flux density at ground and the right bottom panel, the absorbed power through the whole atmosphere. Note that all plots show the shape of the incoming solar radiation which depends on solar zenith angle. See text for the explanation of the features.

Title Page

Abstract

Introduction

Conclusions

References

Tables

Figures

⏪

⏩

◀

▶

Back

Close

Full Screen / Esc

Printer-friendly Version

Interactive Discussion